SEE PROJECT FOR TESTING GRAVITY IN SPACE: CURRENT STATUS AND NEW ESTIMATES

A.D. Alexeev, K.A. Bronnikov, N.I. Kolosnitsyn, M.Yu. Konstantinov, V.N. Melnikov¹† and A.J. Sanders²‡

† RGS, 3-1 M. Ulyanovoy St., Moscow 117313, Russia

‡ Dept. of Physics and Astronomy, University of Tennessee, Knoxville, TN 37996-1200, USA

Received 20 December 1998

We describe some new estimates concerning the recently proposed SEE (Satellite Energy Exchange) experiment for measuring the gravitational interaction parameters in space. The experiment entails precision tracking of the relative motion of two test bodies (a heavy "Shepherd", and a light "Particle") on board a drag-free capsule. The new estimates include (i) the sensitivity of Particle trajectories and G measurement to the Shepherd quadrupole moment uncertainties; (ii) the measurement errors of G and the strength of a putative Yukawa-type force whose range parameter λ may be either of the order of a few metres or close to the Earth radius; (iii) a possible effect of the Van Allen radiation belts on the SEE experiment due to test body electric charging.

1. Introduction

The SEE (Satellite Energy Exchange) concept of a space-based gravitational experiment was suggested in the early 90s [1] and was aimed at precisely measuring the gravitational interaction parameters: the gravitational constant G, possible violations of the equivalence principle measured by the Eötvös parameter η , time variations of G, and hypothetical non-Newtonian gravitational forces (parametrized by the Yukawa strength α and range λ). Such tests are intended to fill gaps left by current methods of ground-based experimentation and observation of astronomical phenomena. The significance of new measurements is quite evident since nearly all modified theories of gravity and unified theories predict some violations of the Equivalence Principle (EP), either by deviations from the Newtonian law (inverse-square-law, ISL) or by composition-dependent (CD) gravity accelerations, due to the appearance of new possible massive particles (partners); time variations of G are also generally predicted [2, 3].

The idea of the SEE method is to study the relative motion of two bodies on board a drag-free Earth satellite using horseshoe-type trajectories, previously known in planetary satellite astronomy: if the lighter body (the "Particle") is moving along a lower orbit than the heavier one (the "Shepherd") and approaching from behind, then the Particle almost overtakes the Shepherd, but it gains energy due to their gravitational interaction, passes therefore to a higher orbit and begins to lag

¹e-mail: melnikov@rgs.phys.msu.su

²e-mail: asanders@utkux.utcc.utk.edu

behind. The interaction phase can be studied within a drag-free capsule (a cylinder up to 20 m long, about 1 m in diameter) where the Particle can loiter as long as 10^5 seconds. It was claimed that the SEE method exceeded in accuracy all other suggestions, at least with respect to G and α for λ of the order of metres. Some design features were considered, making it possible to reduce various sources of error to a negligible level. It was concluded, in particular, that the most favourable orbits are the sun-synchronous, continuous sunlight orbits situated at altitudes between 1390 and 3330 km.

Since the origination of the SEE concept, the development has focused on critical analyses and critical hardware requirements. All indications from this work are that the SEE concept is feasible and practicable [4]. A "blue ribbon" Theory Advisory Group, formed two years ago to critique Project-SEE activities and goals, has concluded that they are sound.

This paper presents some new evaluations concerning the opportunities of the SEE concept and its yet-unresolved difficulties. In Sec. 2, for comparison, we briefly outline the current status of terrestrial and astronomical determination of the gravitational interaction parameters to be measured by the SEE method. In Sec. 3, on the basis of computer simulations of Particle trajectories, we estimate the requirements for the Shepherd quadrupole moment uncertainty. Sec. 4 shows the results of simulations of the measurement procedure itself, which enables us to estimate the possible measurement accuracy with respect to G and α for λ of the order of either metres or the Earth's radius. Sec. 5 discusses a spurious effect of test body electric charging

when the satellite orbit passes through the Van Allen radiation belts, rich in high-energy protons. Sec. 6 is a conclusion.

In what follows, the term "orbit" applies to satellite (or Shepherd) motion around the Earth, while the words "trajectory" or "path" apply to Particle motion with respect to the Shepherd inside the capsule.

2. State of the art: a brief survey

Since gravitational forces are so very small, precision-measurement techniques have been at the core of terrestrial gravity research for two centuries. However, evidence is increasingly accumulating which indicates that terrestrial methods have plateaued in accuracy and are unlikely to achieve significant accuracy gains in the future [5]. For example, the uncertainty in the gravitational constant G had been accepted as 128 ppm for nearly two decades, and the actual uncertainty in G—as indicated by the scatter of results among recent experiments which claim high accuracy— is roughly the same (about 140 ppm). We discuss below the situation with respect to several key measurements.

2.1. Terrestrial determinations of G

The Luther & Towler determination of G in 1982 [6], with the result $(6.6726 \pm 0.0005) \cdot 10^{-11}$ N·m²/kg² and other, less precise experiments gave rise to the current official CODATA value of G, viz. $6.67259 \cdot 10^{-11}$ N·m²/kg² with an error of 128 ppm. Several still other experiments which also claimed high precision were ignored by CODATA because of inadequate documentation of systematic errors.

There is considerable evidence that the uncertainty in G has plateaued at about 100 ppm. At a recent (November 23–24, 1998) conference in London, several new (1998) determinations of G were reported. The obtained values for G (in units of $10^{11}~{\rm N\cdot m^2/kg^2}$) and their estimated error $\delta G/G$ in ppm are as follows:

Fitzgerald and Armstrong (New Zealand) [7]	$6.6742 \\ 6.6746$	90 134
Nolting et al. (Zurich) [8]	6.6749	210
Meyer et al. (Wuppethal) [9]	6.6735	240
Karagioz et al. (Moscow) [10]	6.6729	75
CODATA (1986)	6.67259	128

Obviously, most of the stated errors are of the order 100 ppm. Moreover, the scatter (1-sigma) about the mean is about 140 ppm. Some of the investigators still hope for accuracy of 10 ppm. It remains to be seen whether they will be able to report error estimates of this size or, more importantly, whether their respective values for G will actually agree within 10 ppm.

We note that this analysis is perhaps unduly optimistic since it excludes one extremely bad outlier: the very careful and well documented experiment by the Physikalisch-Technische Bundesanstalt in the late 1980s and early 1990s, which obtained a series of values for G that were consistenly above the results of most experimenters by about 6000 ppm $(0.6\,\%\,!)$, while claiming an error of about 100 ppm [13]. No explanation for such a large discrepancy has been found.

It might seem that the problems of terrestrial apparatus must inexorably yield to new technologies — that the promise of ever increasing sensitivities would also lead to ever improving accuracy. However, this may not be true, since it is various systematic errors which limit the ultimate attainable accuracy in terrestrial experiments [5].

2.2. Terrestrial tests of the equivalence principle (EP) and search for Yukawa forces

The EP may be tested by searching for either violations of the inverse-square law (ISL) or composition-dependent (CD) effects in gravitational free fall.

In the watershed year of 1986, Fischbach startled the physics community by showing that Eötvös's famous turn-of-the-century experiment is much less decisive as a null result than was generally believed [14]. Prior to this time, experiments by Dicke [15] and Braginsky [16] had demonstrated the universality of free fall (UFF) to very high accuracy with respect to several metals falling in the gravitational field of the Sun (the Eötvös parameter η was ultimately found to be smaller than 10^{-12}). The interpretation of these results at the time was that they validated UFF.

It was implicit that any violation would have infinite range, like gravity [17]. During the 1970s and early 1980s there was also a flurry of activity concerning possible ISL violations, which eventually led to null results at the levels of precision then available (Fujii, [18], Long [19]).

Since 1986 it has become customary to parametrize possible apparent EP violations as if due to a Yukawa particle with a Compton wavelength λ . This approach unites both ISL and CD effects very naturally, while the parameter values in the Yukawa potential suggest which experimental conditions are required to detect the new interaction.

Following Fischbach's conjecture, ISL and CD tests were undertaken by many investigators. Although a number of anomalies were initially reported, nearly all of these were eventually explained in terms of overlooked systematic errors or extreme sensitivity to models, while most investigators obtained null results. By far the tightest bounds are those obtained by Adelberger and his "Eot-Wash" group at the University of Washington [20]. This group expects a further improve-

ment of at least an order of magnitude [21]. A positive result for a deviation from the Newtonian law (ISL) was obtained (and interpreted in terms of a Yukawatype potential) in the range of 20 to 500 m by Achilli and colleagues [22]; this needs to be verified in other independent experiments.

For reviews of terrestrial searches for non-Newtonian gravity, see [17, 23, 24]. The opportunities of the SEE concept in this respect are discussed in Refs. [1, 4] and in the present paper.

The UFF is still in the scope of the current experimental projects, and the SEE concept suggests here a progress of 3 to 4 orders of magnitude as compared with Ref. [16]. Only one project, STEP (Satellite Test of the EP) promises a greater progress but meets some significant problems of its own [25], connected, in particular, with the radiation belts.

3. Simulations of Particle trajectories and the Shepherd quadrupole moment

In the previous studies of the SEE project it was assumed that the capsule was about 20 m long and the initial Shepherd-Particle separation x_0 along the capsule axis was as great as 18 m; some estimations were also made for 5 m $\leq x_0 \leq$ 10 m. The Shepherd mass was taken to be M=500 kg and the Particle mass m=0.1 kg. The present study retains these values.

In what follows we describe some characteristic features of Particle trajectories with a goal to determine their sensitivity to the uncertainty of the Shepherd quadrupole moment J_2 for $x_0 \geq 5$ m. As in our previous studies, the capsule diameter is supposed to be 1 m.

The reason for considering the quadrupole moment uncertainty is technological by origin. Namely, it is hard to produce a spherically symmetric Shepherd to a required accuracy and, instead, it has been suggested [1] to use a Cook-Marussi stack of cylinders with $J_2 > 0$, which may be manufactured more easily. A slow rotation of the Shepherd with $J_2 > 0$ will stabilize its position and orientation.

The value of J_2 can be provided with some uncertainty δJ_2 . To avoid the inclusion of δJ_2 in the set of parameters to be determined in the experiment, it is useful to know which values of δJ_2 will be negligible, since the growth of the number of parameters leads to serious problems in data processing.

3.1. Equations of motion and the initial data

Assuming that the relative motion of the test bodies inside the capsule occurs in the satellite orbital plane, the reduced Lagrangian of the Particle motion reads

$$L = \frac{M}{2}(\dot{R}^2 + R^2\dot{\varphi}^2)$$

$$+\frac{m}{2}\left[\dot{r}^2 + r^2(\dot{\varphi} + \dot{\psi})^2\right] + G\frac{M_{\oplus}m}{r} + G\frac{Mm}{s}\left\{1 + J_2\left(\frac{r_s}{s}\right)^2 P_2(\cos\theta)\right\} \left(1 + \alpha e^{-s/\lambda}\right)$$
(1)

where (R,φ) are the Earth-centred polar coordinates of the Shepherd in the orbital plane; $r=\sqrt{(R+y)^2+x^2}$ and ψ are the Earth-centred polar coordinates of the Particle; x and y are the Shepherd-centred Particle coordinates, where x is the "horizontal" one, i.e., along the orbit and simultaneously along the capsule and y is the "vertical" one, along the Earth-Shepherd radius vector; $s=\sqrt{x^2+y^2}$ is the Particle-Shepherd separation; M_{\oplus} , M and m are the Earth, Shepherd and Particle masses, respectively; J_2 is the quadrupole moment of the Shepherd, r_s is its radius and P_2 is the Legendre polynomial

$$P_2(\cos\theta) = \frac{3\cos^2\theta - 1}{2},$$

where θ is the angle between the line connecting the centres of the test bodies and the Shepherd equatorial plane. It is easy to see that if the Shepherd symmetry axis is in its orbital plane, then $\theta = \theta_0 = -\arctan(y/x) + \varphi$. If the symmetry axis of Shepherd is orthogonal to its orbital plane, then $\theta = 0$. In general, if χ is the angle between the Shepherd symmetry axis and its orbital plane, then $\theta = \theta_0 \cos \chi$. Hence the influence of J_2 on the Particle motion is minimum if the Shepherd symmetry axis lies in its orbital plane and is maximum if they are mutually orthogonal.

For simplicity (and taking into account the corresponding estimate) we neglect the influence of the Particle on the Shepherd, so the Shepherd trajectory is considered to be given. Then, varying the above Lagrangian with respect to x and y, taking into account that $M\gg m$ and $R\gg s$, we arrive at the following equations of Particle motion with respect to the Shepherd:

$$\frac{d^2x}{dt^2} = 2\dot{y}\dot{\varphi} + x\left\{\dot{\varphi}^2 - \frac{GM_{\oplus}}{r^3}\right\} - \frac{2\dot{R}\dot{\varphi}y}{R}$$

$$-\frac{G\overline{M}}{s^3}x\left\{1 + J_2\left(\frac{r_s}{s}\right)^2 P_2(\cos\theta)\right\}$$

$$-\alpha x\frac{G\overline{M}}{s^2}\left\{1 + J_2\left(\frac{r_s}{s}\right)^2 P_2(\cos\theta)\right\}\left(\frac{1}{s} + \frac{1}{\lambda}\right)e^{-s/\lambda}$$

$$-\frac{G\overline{M}r_0^2}{2s^5}J_2\left(1 + \alpha e^{-s/\lambda}\right) \times \left[x(1 + 3\cos 2\theta) + 3y\sin 2\theta\cos\chi\right] \qquad (2)$$

$$\frac{d^2y}{dt^2} = -2\dot{x}\dot{\varphi} + (R + y)\left\{\dot{\varphi}^2 - \frac{GM_{\oplus}}{r^3}\right\} + \frac{2\dot{R}\dot{\varphi}x}{R}$$

$$-\frac{G\overline{M}}{s^3}y\left\{1 + J_2\left(\frac{r_s}{s}\right)^2 P_2(\cos\theta)\right\}$$

$$-\alpha y\frac{G\overline{M}}{s^2}\left(\frac{1}{s} + \frac{1}{\lambda}\right)\left\{1 + J_2\left(\frac{r_s}{s}\right)^2 P_2(\cos\theta)\right\}e^{-s/\lambda}$$

$$+\frac{G\overline{M}r_0^2}{s^5}J_2\left(1+\alpha e^{-s/\lambda}\right) \times \times \left[3x\sin 2\theta\cos\chi + y(1-3\cos\theta)\right]$$
(3)

where $\overline{M} = M + m$.

Two kinds of initial conditions for Eqs. (2) and (3) were used during the simulations. First, we used the so-called "standard" initial conditions, taking the Particle velocity components $\dot{x}(0)$ and $\dot{y}(0)$ corresponding to its unperturbed (i.e., without the M-m interaction) orbital motion distinguished from the Shepherd's orbit only by its radius (for circular orbits) or major semiaxis (for elliptic orbits). Assuming that the Particle motion begins right at the moment when the Shepherd passes its perigee, these conditions have the form

$$x(0) = x_0, y(0) = y_0,$$

$$\dot{x}(0) = \frac{\omega e' y_0}{2(1-e)^2}, \dot{y}(0) = -\frac{\omega e x_0}{e'(1-e)}$$
(4)

where $\omega^2 = GM_{\oplus}/R_0^3$, R_0 is the Shepherd orbital radius (at the perigee), e is the orbital eccentricity and $e' = \sqrt{1 - e^2}$.

For clearness, the relations (4) are written in the linear approximation in the variables x and y. Higher-order approximations were used in the simulation process as well.

The second kind of initial conditions correspond to small variations of initial velocities with respect to their "standard" values.

The set of equations (2)–(3) was solved numerically using the software developed previously [4] to analyze the SEE project.

On the basis of numerical solution of Eqs. (2) and (3), we considered two types of Particle trajectories, corresponding to different choices of the initial data: (i) approximately U-shaped ones and (ii) cycloidal ones, containing loops (see more details on the trajectories in [1, 4]), for orbital altitudes $H_{\rm orb} = 500$, 1500 and 3000 km. The uncertainty δJ_2 ranged in the interval $10^{-3} \div 10^{-5}$; and initial Particle position changed in the range 6 m $\leq x_0 \leq 18$ m, -25 cm $\leq y_0 \leq -5$ cm.

For $H_{\rm orb}=500$ km, all U-shaped paths contained a sinusoidal component (with the orbital frequency), starting at $x_0 \leq 8$ m, while for $H_{\rm orb}=1500$ and 3000 km it was present in paths starting at $x_0 \leq 10$ m. In other families of U-shaped trajectories a sinusoidal component was present only in the case $|y_0| \geq 20$ cm.

3.2. Restrictions on the Shepherd quadrupole moment uncertainty

Small Shepherd quadrupole moment uncertainties δJ_2 create small displacements $\delta \vec{r}$ of a Particle trajectory with respect to unperturbed one, $\vec{r}_0(t)$:

$$\delta \vec{r} = \vec{r}_i(t) - \vec{r}_0(t)$$

where \vec{r}_j is the perturbed path. Instead of the full displacement $\delta \vec{r}$, a displacement δx along the x axis

Table 1. Displacements of U-shaped trajectories under $\delta J_2 = 10^{-4}$ for the Shepherd symmetry axis in its orbital plane. The second line shows x_0 .

y_0	$\delta x_{\rm max} \times 10^7 \; (\rm m)$				
(cm)	18 m	10 m	8 m	6 m	4 m
-25	13.3	7.52	7.98	8.57	14.90
-20	5.51	4.65	4.83	5.51	5.84
-15	1.98	2.87	3.03	3.3	2.18
-10	0.56	1.59	1.7	1.88	0.66
- 5	0.11	0.59	0.62	0.69	0.14

Table 2. Displacements of U-shaped trajectories under $\delta J_2 = 10^{-4}$ for the Shepherd symmetry axis orthogonal to its orbital plane. The second line shows x_0 .

y_0	$\delta x_{\rm max} \times 10^7 \; ({\rm m})$				
(cm)	18 m	10 m	8 m	6 m	4 m
-25	54.2	62.4	68.9	81	57
-20	21.9	25.8	28.1	32.2	23.3
-15	7.94	10.2	11.5	14	8.7
-10	2.25	3.42	4.15	5.45	2.65
- 5	0.45	0.83	1.05	1.47	0.58

may be considered since, by numerical simulations, displacements along the y axis are an order of magnitude smaller than δx .

Numerical simulations show that in the whole range of the above initial conditions the displacement δx is (as it should naturally be) a linear function of δJ_2 ; for $\delta J_2 = 10^{-4}$. For the case when the Shepherd symmetry axis is located in the orbital plane, the maximum values of δx for U-shaped trajectories are given in Table 1.

One can conclude that, if the distance measurement error is 10^{-6} m, for most of the trajectories the uncertainty $\delta J_2 = 10^{-4}$ is admissible.

The increase of δx for small values of $|y_0|$ is explained by a large displacement of the turning point towards the Shepherd.

When the Shepherd symmetry axis is orthogonal to the orbital plane, these estimations change as shown in Table 2.

For cycloidal trajectories these values are approximately an order of magnitude smaller than those for the U-shaped ones.

It was also found that δx decreases with increasing orbital altitude $H_{\rm orb}$. Table 3 shows, as an example, the displacements of U-shaped trajectories with $x_0=18$ m for $H_{\rm orb}=500$, 1500 and 3000 km and the Shepherd symmetry axis located in its orbital plane.

Table 3. Displacements of U-shaped trajectories with $x_0 = 18$ m and different orbital altitudes for $\delta J_2 = 10^{-4}$. The second line shows the values of $H_{\rm orb}$.

y_0	$\delta x_{\rm max} \times 10^7 \; ({\rm m})$				
(cm)	500 km	1500 km	3000 km		
-25	42.6	13.3	4.84		
-20	11.9	5.51	2.18		
-15	4.02	1.98	0.86		
-10	1.03	0.56	0.28		
-5	0.17	0.11	0.07		

The above results show that the Shepherd quadrupole moment uncertainty δJ_2 may be neglected in the SEE experiment with circular Shepherd orbits at $H_{\rm orb}=1500$ or 3000 km and U-shaped Particle trajectories if $\delta J_2 \leq 10^{-5}$ and the position measurement error δl is 10^{-6} cm, or $\delta J_2 \leq 10^{-7}$ for $\delta l=10^{-8}$ cm. For cycloidal Particle trajectories or elliptic Shepherd orbits these estimates become $\delta J_2 \leq 10^{-4}$ and $\delta J_2 \leq 10^{-6}$, respectively. For low orbits, $H_{\rm orb}=500$ km, the resitrictions on δJ_2 become more stringent: $\delta J_2 \leq 10^{-6}$ for $\delta l=10^{-6}$ cm and $\delta J_2 \leq 10^{-8}$ for $\delta l=10^{-8}$ cm. However, as is evident from the above tables, these requirements may be relaxed by an order of magnitude if one discards some trajectories.

The influence of δJ_2 on the accuracy of G measurement may be now estimated as follows. Let some value of δJ_2 produce the trajectory displacement $|\delta \vec{r}| \leq \delta l_j$ while the variation δG_0 of G with the same initial conditions gives the trajectory displacement $|\delta \vec{r}| \leq \delta l_G$. Then, keeping in mind the linear dependence of trajectory displacements on δJ_2 and δG , the accuracy of G measurement under the uncertainty δJ_2 may be estimated as

$$\frac{\delta G}{G} \le \frac{\delta l_j}{\delta l_G} \frac{\delta G_0}{G}.$$

Using this inequality and the results of trajectory simulations, we obtain the following estimates for U-shaped Particle trajectories in circular orbits with $H_{\rm orb} = 1500$ km:

Table 4. Estimates of $\delta G/G$ in ppm for $\delta J_2 = 10^{-4}$, when the symmetry axis of the Shepherd lies in $(\chi = 0)$ or is ortogonal to $(\chi = \pi/2)$ its orbital plane. The second line shows x_0 .

y_0 ,	$\chi =$	= 0	$\chi =$	$\pi/2$
$^{ m cm}$	18 m	6 m	18 m	6 m
-25	0.88	0.7	3.57	6.7
-20	0.27	0.3	1.05	1.73
-15	0.06	0.1	0.24	0.44

One can conclude that the uncertainties $\delta J_2 \lesssim 10^{-5}$ do not create substantial G errors for most of the trajectories.

4. Simulations of experimental procedures

This section describes the results of computer simulations of the whole measurement procedures aimed at obtaining the sought-after gravitational interaction parameters. These simulations assumed the Shepherd mass M=500 kg, a circular orbit with $H_{\rm orb}=1500$ km under a spherical gravitational potential of the Earth, and a Particle mass of 100 g. Where relevant, it is assumed that both the Shepherd and the Particle are made of tungsten. Their identical compositions are assumed for simplicity since this work is performed only for estimation purposes.

4.1. Equations of motion with Yukawa terms

We will begin with a presentation of the Particle equations of motion in the relevant approximation, including the contributions from hypothetical Yukawa forces, taking into account the finite size of the Yukawa field sources.

Let the interaction potential for two elementary masses m_1 and m_2 be described by the potential

$$dV^{\text{Yu}} = \frac{G \, dm_1 dm_2}{r} \alpha \, e^{-r/\lambda} \tag{5}$$

where r is the masses' separation, α and λ are the strength parameter and the range of the Yukawa forces. Then for two massive bodies with the radii R_1 and R_2 after integration over their volumes we obtain [26]

$$V^{\text{Yu}} = \frac{G m_1 m_2 \beta_1 \beta_2}{r} \alpha e^{-r/\lambda}$$
 (6)

where

$$\beta_i = 3 \left(\frac{\lambda}{R_i}\right)^3 \left[\frac{R_i}{\lambda} \cosh \frac{R_i}{\lambda} - \sinh \frac{R_i}{\lambda}\right]. \tag{7}$$

When $R_i/\lambda \ll 1$, we have $\beta_i \approx 1$. This may be the case when we consider the interaction between the Shepherd and the Particle at a distance of the order of a few metres. The radii of the Shepherd and the Particle are small: $R_1 \approx 18$ cm for the Shepherd and $R_2 \approx 1.1$ cm for the Particle. If the range λ is of the order of the Earth radius, $\lambda \approx R_{\oplus}$, we have $\beta_{\oplus} = 1.10$ and $\beta_{1,2} = 1$ where the indices 1 and 2 label the Shepherd and the Particle, respectively.

The equations of motion are obtained under the following assumptions. There are two Yukawa interactions with the parameters λ_0 and α_0 referring to the Earth-Shepherd and Earth-Particle interactions which are the same (due to the assumed identical composition for the Shepherd and the Particle), while λ and α determine the Shepherd-Particle interaction. The equations of motion in the frame of reference connected with

the Shepherd, with the same notations x, y, s as previously, are

$$\ddot{x} + 2\omega^{2}\dot{y} + G(m_{1} + m_{2})\frac{x}{s^{3}} - 3\omega^{2}\frac{xy}{s} + G(m_{1} + m_{2})\frac{x}{s^{3}}\alpha\left(1 + \frac{s}{\lambda}\right)e^{-s/\lambda} = 0;$$

$$\ddot{y} - 2\omega\dot{x} - 3\omega^{2}y + G(m_{1} + m_{2})\frac{y}{s^{3}} + \frac{3\omega^{2}}{r_{01}}\left(y^{2} - \frac{x^{2}}{2}\right) + G(m_{1} + m_{2})\frac{y}{s^{3}}\alpha\left(1 + \frac{s}{\lambda}\right)e^{-s/\lambda} - \omega^{2}\beta_{0}\alpha_{0}e^{-r_{01}/\lambda_{0}}y = 0$$
(8)

where ω is the orbital frequency:

$$\omega^2 = \frac{GM_{\oplus}}{r_{01}^3} \left[1 + \beta_0 \alpha_0 \left(1 + \frac{r_{01}}{\lambda_0} \right) e^{-r_{01}/\lambda_0} \right]. \tag{9}$$

We have neglected the terms quadratic in s/r_{01} times α or α_0 due to their manifestly small contributions.

If we set $\alpha_0 = 0$ in Eqs. (8), we obtain the equations used to describe only the Shepherd-Particle Yukawa interaction. One can notice that Yukawa terms are roughly proportional to the gradients of the corresponding Newtonian accelerations, namely, Gm_1/s^3 for the Shepherd-Particle interaction and $GM_{\oplus}/r_{01}^3 \approx \omega^2$ for (say) the Earth-Shepherd interaction. In our case these quantities are estimated as

$$\frac{Gm_1}{s^3} \approx 2.7 \cdot 10^{-10} \text{ s}^{-2}$$
 for $s = 5 \text{ m}$,
 $\omega^2 \approx 8.16 \cdot 10^{-7} \text{ s}^{-2}$. (10)

Thus, given the same strength parameter, the Earth's Yukawa force is three orders of magnitude greater than that between the Shepherd and the Particle, therefore one might expect some significant progress in an ISL test for λ of the order of the Earth's radius.

The effect of the Earth's Yukawa force is proportional to the displacements of the statellite along the direction of the Earth's radius. Therefore the sensitivity of the SEE method will increase if one uses orbits with eccentricities of the order of 0.01, following Nordtvedt's suggestion [27]. (Larger eccentricities would too much disturb the qualitative picture of a SEE encounter.) Tentative estimates show that in this way one can achieve sensitivities to $\alpha \sim 10^{-10}$, and more thourough studies are in progress.

Eqs. (8) were used to simulate the measurement procedures.

4.2. Simulations of an experiment for measuring G

The constant G is determined from the best fitting condition between the "theoretical" $(\vec{r}^{\,\text{th}}(t_i) = \vec{r}_i^{\,\text{th}})$ and "empirical" (\vec{r}_i) Particle trajectories near the Shepherd. The fitting quality is evaluated by minimizing a

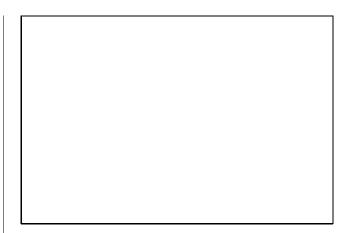


Figure 1: Errors δG estimated by the gradient descent $(R_{\rm grad})$ and consecutive descent $(R_{\rm s})$ methods

functional characterizing a "distance" between the trajectories. We have considered the following functionals for such "distances":

$$S = \sum_{i=1}^{N} \left[(x_i - x_i^{\text{th}})^2 + (y_i - y_i^{\text{th}})^2 \right], \tag{11}$$

$$S_x = \sum_{i=1}^{N} (x_i - x_i^{\text{th}})^2, \qquad S_y = \sum_{i=1}^{N} (y_i - y_i^{\text{th}})^2, \quad (12)$$

$$S^* = \sum_{i=1}^{N} \left[|x_i - x_i^{\text{th}}| + |y_i - y_i^{\text{th}}| \right], \tag{13}$$

$$S_x^* = \sum_{i=1}^{N} |x_i - x_i^{\text{th}}|, \qquad S_y^* = \sum_{i=1}^{N} |y_i - y_i^{\text{th}}|.$$
 (14)

The theoretical trajectory depends on the gravitational constant G, on the initial coordinates x_0, y_0 and on the initial velocities v_{x0}, v_{y0} . To estimate G, one chooses the value for which a "distance" functional in the space of the five variables $(G, x_0, y_0, v_{x0}, v_{y0})$ reaches its minimum.

We carried out a computer simulation of the SEE experiment and estimated δG for a given coordinate measurement error ($\sigma = 1 \cdot 10^{-6}$ m). As "empirical" trajectories, we took computed trajectories, with specified values of the above five variables, where a Gaussian noise was introduced from a random number generator. Independent "empirical trajectories were created by non-intersecting random number sequences. The functional was minimized using the gradient descent method and the consecutive descent method. The starting value of the "vertical" (along the Earth's radius) coordinate, y_0 , was taken to be 0.25 m, while the horizontal one, x_0 , varied between 2 and 18 m. Fig 1 shows the dependence of the errors $\delta G/G = R_{\rm grad}$, obtained by the gradient descent method and $\delta G/G = R_s$, obtained by the consecutive descent method. All the errors are estimated by confidence intervals corresponding



Figure 2: The SEE method sensitivity to Yukawa forces between the Shepherd and the Particle

to a confidence of 0.95. The mean values of these errors are as follows:

$$R_{\rm grad} = 4.69 \cdot 10^{-8}, \qquad R_{\rm s} = 5.24 \cdot 10^{-8}.$$

Thus the errors estimated by the gradient and consecutive descent methods are close to each other and are about an order of magnitude smaller than the error from one-trajectory data. It has been discovered that the simulation results strongly depend on the random number generator, so that ordinary generators are not perfect.

The use of truncated functionals like (2) has shown that a functional incorporating the more informative "horizontal" coordinate x leads to estimates close to those obtained from the total functional, whereas the use of y alone substantially decreases the sensitivity. Therefore in practice, to determine G, it is sufficient to measure only one of the two coordinates, viz. x.

Since the "empirical" trajectory is built on the basis of a computed one, with a known value of the gravitational constant G_0 , it appears possible to estimate a possible systematic error inherent in the data processing method. The latter has turned out to be in most cases much smaller than the random error. This result shows the correctness of the methods used.

As is evident from the results, the best accuracy is achieved at values of x_0 (\approx the capsule size) about 4–5 metres.

4.3. Sensitivity to Yukawa forces with $\lambda \sim 1~\text{m}$

In an experiment for finding a Yukawa interaction between the Shepherd and the Particle with the potential (6) with $\beta_{1,2} = 1$, one computes two theoretical trajectories: one ignoring the Yukawa forces $(x^0(t_i), y^0(t_i))$ and another taking them into account $(x^{\alpha}(t_i), y^{\alpha}(t_i))$.



Figure 3: The SEE method sensitivity to Yukawa forces with the range parameter λ_0 of the order of the Earth's radius R_{\oplus}

These two computed curves are compared with the empirical trajectory using the functional S_k ($k=0,\alpha$) according to (11) which may be considered as a dispersion characterizing a scatter of the "empirical" coordinates with respect to the fitting trajectory. This is true when the theoretical model is adequate to the real situation. In the case $k=\alpha$ the functional $S_k=s_\alpha$ has a χ^2 distribution with $n_2=2N-1$ degrees of freedom. With k=0 the parameter α is absent, therefore S_0 is distributed according to the χ^2 law with $N_1=2N$ degrees of freedom. Then their ratio $S_0/S_\alpha=F_{n_2,n_1}$ will be distributed according to the Fischer law with n_2 and n_1 degrees of freedom. If an experiment shows that, on a given significance level q, the relation

$$S_0/S_\alpha \ge F_{n_1,n_2,q} \tag{15}$$

is valid, one should conclude that a Yukawa force has been detected. An equality sign shows a minimum detectable force on the given significance level q. We have assumed q=0.95. The results of a sensitivity computation for different values of the space parameter λ are presented in Fig. 2.A maximum sensitivity of $\alpha=2.1\cdot 10^{-7}$ has been observed for $\lambda=1.25$ m. This value is 3 to 4 orders of magnitude better than the sensitivity of terrestrial experiments in the same range.

These results are based on the measurement method which was proposed in the original SEE paper [1]; as already mentioned, a method involving an eccentric orbit [27], is much more sensitive and, by our tentative estimates, can give an error $\delta \alpha \lesssim 10^{-10}$.

4.4. Sensitivity to Yukawa forces with $\lambda \sim R_{\oplus}$

To estimate the parameter α_0 in Eqs. (8), computer simulations were carried out using the method as de-

scribed above for α , based on the Fischer criterion for the significance level 0.95. The range parameter λ_0 varied from $(1/32)R_{\oplus}$ to $32R_{\oplus}$. Two trajectories with the initial Shepherd-Particle separations x_0 of 2 and 5 m were calculated. In both cases the impact parameter y_0 was chosen to be 0.25 m. We used Eqs. (8) with $\alpha = 0$, i.e., excluding the non-Newtonian interaction between the Shepherd and the Particle. As is evident from Eqs. (8), the Particle trajectory depends on the ratio r_{01}/λ_0 in the product $(r_{01}/\lambda_0) e^{-r_{01}/\lambda_0}$. This quantity reaches its maximum at $\lambda_0 = r_{01}/2$. Our calculations have confirmed that a maximum sensitivity of the SEE method $(3.4 \cdot 10^{-8} \text{ for } x_0 = 5 \text{ m})$ is indeed observed at this value of λ_0 . This is about an order of magnitude better than the estimates obtained by other methods. Hopefully this estimate may be further improved by about an order of magnitude by optimisation of the orbital parameters. However, there is a factor which can, to a certain extent, spoil these results, namely, the uncertainty in the parameter ω which, in this calculation, was assumed to be precisely known.

The simulation results are shown in Fig. 3 for two trajectories with initial Shepherd-Particle separations of 2 and 5 metres.

5. A possible effect of the Earth's radiation belt

Charged particles, penetrating into the SEE capsule from space and captured by the test bodies, create electrostatic forces that could substantially distort the experimental results. Among the sources of such particles one should mention (i) cosmic-ray showers, (ii) solar flares and (iii) the Earth's radiation belts (Van Allen belts). The effect of cosmic-ray showers was estimated in Ref. [1] and shown to be negligible. Solar flares are more or less rare events and, although they create very significant charged particle fluxes, sometimes even exceeding those in the most dense regions of the radiation belts, one can assume that the SEE measurements (except those of G) are stopped for the period of an intense flare. On the contrary, the effect of the Van Allen belts is permanent as long as the satellite orbit passes, at least partially, inside them.

We will show here that the charging is unacceptably high at otherwise favourable satellite orbits, so that some kind of charge removal technique is necessary, but this problem may be solved rather easily by presently available technology.

The range of the most favourable SEE orbital altitudes, roughly 1400 to 3300 km [1], coincides with the inner region of the so-called inner radiation belt [28]–[31], situated presumably near the plane of the magnetic equator. This region is characterized by a considerable flux of high-energy protons and electrons. For a SEE satellite at altitudes near 1500 km the duration

of the charging periods is about 12 minutes. Maximum charging rates occur in the central Atlantic. It should be noted that the South Atlantic Anomaly (SAA) — a region of intense Van Allen activity which results from the low altitude of the Earth's magnetic field lines over the South Atlantic Ocean — cannot cause additional problems for the SEE experiments. The reason is that the SAA mostly contains low-energy protons which cannot penetrate into the SEE capsule.

Electrons are known to be stopped by even a thin metallic shell, so only protons are able to induce charges on the test bodies. Proton-induced charges on the test bodies can create considerable forces. The inner radiation belt contains protons with energies of 20 to 800 MeV, and their maximum fluxes at an altitude of 3000 km over the equator are as great as about $3\cdot 10^6\,\mathrm{cm^{-2}s^{-1}}~$ for energies $E\gtrsim 10^6~\mathrm{eV}$ and about $2\cdot 10^4\,\mathrm{cm^{-2}s^{-1}}~$ for $E\gtrsim 10^7~\mathrm{eV}.$ At 1500 km altitude these numbers are a few times smaller; the fluxes gradually decrease with growing latitude φ and actually vanish at $\varphi\sim 40^\circ$.

It is thus necessary to have some estimates taking into account that (i) the capsule walls have a considerable thickness and stop the low-energy part of the proton flux and (ii) among the protons that penetrate the capsule and hit the Particle, the most energetic ones, whose path in the Particle material is longer than the Particle diameter, fly it through and hit the capsule wall again. As for the Shepherd, its size is large enough to stop the overwhelming majority of protons which hit it.

In what follows, we will assume a Shepherd radius of 20 cm and a Particle radius of 2 cm and estimate the captured charges for some satellite orbits in a capsule whose walls of aluminium are 2, 4, 6 and 8 cm thick. The SEE satellite must actually involve several coaxial cylinders for thermal-radiation control, and the combined thickness of their walls must amount to several cm. We will assume, in addition, that the Particle also consists of aluminium and stops all protons whose path is shorter than 4 cm (thus a little overestimating the charge since most of protons will cover a smaller path through the Particle material). A 100 g Particle of aluminium will have a radius of ≈ 2.07 cm.

It is advisable to determine first which charges (and fluxes that create them) might be regarded negligible.

5.1. Admissible charges

Let us estimate the Coulomb interaction both between the Shepherd and the Particle and between each test body and its image in the capsule walls. To estimate the spurious effects on the Particle trajectory, it is reasonable to calculate its possible displacements due to the Coulomb forces from the growing captured charges. We assume that the test bodies are discharged by grounding to the capsule before launching the motion. **Criterion.** We will call the induced charges, or the fields they create, admissible if they cause a displacement of the Particle with respect to the Shepherd smaller than a prescribed coordinate measurement error δl (we take here $\delta l = 10^{-6}$ m) for a prescribed measurement time (we take $t \geq 10^4$ s).

A charge on the Shepherd can be estimated as

$$q_M \approx eS_M \int J(t, x) dt = eS_M F(t, x)$$
 (16)

where e is the elementary charge, x is the capsule wall thickness in cm; J(t,x) is the integral proton flux in cm⁻²s⁻¹ after passing through the wall, that is, the flux of protons with energies $E_p > E_p(x)$ where $E_p(x)$ is such an energy that the proton path in aluminium equals x cm; $S_M \approx 1256$ cm² is the Shepherd's cross-section; F(t,x) is the fluence, i.e., the total number of protons of relevant energies that crosses a square centimeter of area for a certain period t.

In a similar way, the charge captured by the Particle may be found as

$$q_m \lesssim eS_m \int [J(t,x) - J(t,x+4)] dt$$

= $eS_m [F(t,x) - F(t,x+4)]$ (17)

where $S_m \approx 12.56~{\rm cm}^2$ is the Particle cross-section. The subtraction in the square brackets takes into account the protons which fly through the Particle without stopping there. The sign \lesssim is used since the effective Particle cross-section is smaller than its equatorial section.

The Coulomb acceleration $a_Q(t) = q_M q_m/(r^2 m)$ (in the Gaussian system of units) depends on the Shepherd-Particle separation r and on the form of the function J(t), which in turn depends on the satellite orbital motion.

The charge-induced Particle displacement is approximately

$$\Delta l = \int dt \left[\int dt \, a_Q(t) \right] \tag{18}$$

since the acceleration is almost unidirectional. If, for estimation purposes, we suppose that the flux is time-independent, $J=J_0={\rm const.}$, and take into account that in Eq. (17) the difference $J(t,x)-J(t,x+4)\approx \frac{2}{5}J(t,x)$ (or even smaller; see particular values in the next section), then the resulting displacement is about

$$\Delta l \sim \frac{1}{30} \frac{e^2 S_M S_m J_0^2 t^4}{r^2 m}.$$
 (19)

The strong time dependence is explained by the rapid growth of the Coulomb force with capturing the charge. Numerically, with the above values of S_M and S_m , taking m=100 g and r=1 m (the latter leads to an overestimated force since the Particle spends most of time at greater distances), one gets:

$$J_0^2 t^4 \lesssim 0.83 \cdot 10^{18} \text{ s}^2 \text{cm}^{-4}.$$
 (20)

For $t = 10^4$ s an admissible flux is only within 9 cm⁻²s⁻¹.

Another undesired effect is that the Particle, being charged by the belt protons, will interact with the capsule walls. This is well approximated as an interaction with the Particle's mirror image in the wall, while the latter may be roughly imagined as a conducting plane. Then, assuming that the Particle is at average at about 25 cm from the capsule wall and using the same kind of reasoning as above, we obtain instead of (20)

$$J_0^2 t^4 \lesssim 2.07 \cdot 10^{19} \text{ s}^2 \text{cm}^{-4}$$
 (21)

and an admissible proton flux within 45 cm⁻²s⁻¹ for $t = 10^4$ s.

Some more estimates are of interest: if a charge can be kept smaller than a certain value, then how great may it be to create only negligible displacements? Suppose that there are constant charges on both the Shepherd $(q = q_M)$ and the Particle $(q = q_m, m = 100 \text{ g})$, then they are admissible according to the above criterion as long as

$$q_M q_m < 2 \cdot 10^{-6} \text{ CGSE}_q^2 = \frac{2}{9} \cdot 10^{-24} \text{ C}^2,$$
 (22)

$$q_m^2 < \frac{1}{2} \cdot 10^{-6} \, \text{CGSE}_a^2$$
. (23)

These inequalities follow, respectively, from considering the Shepherd-Particle interaction and the interaction between the Particle (located at 25 cm from the wall) and its image. Thus the maximum admissible Particle charge is about $7 \cdot 10^{-4} \ \mathrm{CGSE}_q \approx 1.5 \cdot 10^6 e$; assuming this value, it follows from (22) that the maximum Shepherd charge is about $3 \cdot 10^{-3} \ \mathrm{CGSE}_q \approx 5.5 \cdot 10^6 e$. With these charge values the electric potentials on the test body surfaces are

$$U_M \approx 1.5 \cdot 10^{-4} \,\mathrm{CGSE}_q/\mathrm{cm} = 45 \,\mathrm{mV};$$

$$U_m \approx 3.5 \cdot 10^{-4} \,\mathrm{CGSE}_q/\mathrm{cm} = 105 \,\mathrm{mV}. \tag{24}$$

If by any means the requirements (22), (23) are satisfied (e.g., the potentials are kept smaller than the values (24)), the electrostatic effect on the Particle trajectory may be neglected.

The Shepherd's interaction with its image charge induced in its nearest bottom of the SEE experimental chamber does not lead to appreciable Particle displacements. A very demanding requirements on the Shepherd's charge emerges, however, if the SEE satellite is used for G-dot determination (whose detailed discussion is postponed to future papers). One obtains then

$$U_M \lesssim 12 \text{ mV}.$$
 (25)

Evidently, in this case the Shepherd-Particle interaction per se is not the determining factor with respect to charge limits on the test bodies.

Table 5. Average proton fluxes in some satellite orbits at minimum solar activity (x is given in cm, E_p in MeV; i is the orbit inclination and Ω is its ascension angle, i.e. the longitude at which the satellite crosses the equatorial plane moving northward. The notation 1.2(3) means $1.2 \cdot 10^3$, etc. In the first column, the letter 'a' labels equatorial orbits, 'b' and 'c' mark less and more favourable orbits (that is, with greater and smaller number of protons), respectively, for given altitide and inclination.

					Integral flux for $E_p > E_p(x)$					
Orbit	T	i	Ω	x = 0	x = 2	x = 4	x = 6	x = 8	x = 10	x = 12
	\mathbf{s}			$E_p > 0$	$E_p > 65$	$E_p > 98$	$E_p > 124$	$E_p > 146$	$E_p > 166$	$E_p > 184$
500b	5677	89°	23.7°	1200	8	4.5	3	2.1	1.8	1.5
800a	6053	0°		114	66	51	41	33	28	24
800b	6053	89°	19.4°	2660	71	46	34	26	21	17
1000a	6307	0°		515	325	255	210	165	140	120
1000b	6307	89°	20°	4120	173	116	89	65	54	44
1000c	6307	89°	-83°	51	26	20	16	12	10	8.5
1500a	6960	0°		6905	3160	2360	1850	1470	1260	1070
1500b	6960	102°	-12°	1.2(4)	1420	1000	770	600	500	415
1500c	6960	102°	97°	2264	646	464	365	280	236	196
3000a	9040	0°		2.6(5)	1.7(4)	1.15(4)	9100	6500	5400	4350
3000b	9040	112°	-14.5°	1.6(5)	3700	2400	1750	1300	1060	850
3000c	9040	112°	98°	9.8(4)	3540	2350	1700	1300	1060	850

5.2. Evaluation of charges captured in some orbits

Let us now estimate the charges captured by the Shepherd and the Particle on board a satellite in various circular orbits for a single revolution around the Earth, a period of about two hours. Actual measurement times may exceed this period, but not too much.

Approximate values of time-averaged proton fluxes are presented for some circular orbits in Table 5.

The fluxes in Table 5 have been obtained using the computation software worked out at Nuclear Physics Institute (NPI) of Moscow State University, called SEE2 (Space Environment Effects 2) and SEREIS (Space Environment Radiation Effects Information System) [32]–[34]. This software made use of the NASA models AP8-max and AP8-min for calculating the proton fluxes [35]; however, the latter rest on measurements performed in the solar maximum of 1970 and minimum of 1964, while the NPI software uses some modern models of the Earth's magnetosphere, taking into account its evolution on the scale of decades.

The high-energy particle fluxes in the radiation belts are strongly time-dependent; they vary between maxima and minima of solar activity, being, at least at low altitudes relevant for a SEE mission, greater at solar minima [2–5]. Table 5 shows the fluxes at a solar minimum; similar calculations for a solar maximum show smaller values by at average 20-25 per cent; the difference exceeds this value only for x=0 (being thus greater for low-energy protons than for higher-energy ones).

The solar activity varies from one maximum or minimum to another, the Earth's magnetic field is sensitive to all these variations and also varies due to certain terrestrial phenomena. Another source of uncertainty, probably not a very strong one, is that the shielding effect is calculated by SEE2 software for a detector placed at the centre of a spherical shell of shielding material, whereas the capsule is cylindrical and the angular distribution of the proton flow is also uncertain. It is thus clear that any values like those presented in Table 5 may only serve as a guide, giving correct orders of magnitude.

The above data make it possible to evaluate the captured charges. The results for two orbits, namely, 1500b and 1500c, are presented in Table 6. These are the worst and the best variants of orbits at 1500 km among those analyzed (see the caption of Table 5).

These and other similar data lead to some conclusions of importance for the SEE experiments.

First, the models show zero proton fluxes in equatorial orbits of 500 — 800 km altitudes but indicate considerable fluxes at the same altitudes due to crossing the SAA. It turns out, however, that the SAA is overwhelmingly a low-energy phenomenon and almost does not affect fluxes on the relevant energy scale beginning with approximately 65 MeV. Even more, there is a very small proton flux due to the SAA even at energies over 10 MeV, so that behind a layer of 1 mm the SAA influence is already negligible. Therefore, behind a thicker metal layer there are actually no secondary particles due to SAA protons.

Second, at 1500 km altitude the fluxes substantially depend on the orbit orientation but remain on the same scale of a few million protons per $\rm cm^2$ at energies over 65 MeV.

Orbit	Wall	Average flux,	Peak flux,	Shepherd	Particle
	thickness	${\rm cm}^{-2} {\rm s}^{-1}$	${\rm cm}^{-2} {\rm s}^{-1}$	charge q_M	charge q_m
	2 cm	1420	12300	$1.5 \cdot 10^{10} e$	$4.5 \cdot 10^7 \ e$
1500b	$4~\mathrm{cm}$	1000	8800	$1 \cdot 10^{10} e$	$2.6 \cdot 10^7 e$
	$6~\mathrm{cm}$	770	6800	$7.5 \cdot 10^9 e$	$1.5 \cdot 10^7 \ e$
	8 cm	600	5400	$6 \cdot 10^9 \ e$	$1.2 \cdot 10^7 e$
	$2 \mathrm{~cm}$	646	5700	$6.5 \cdot 10^9 e$	$1.9 \cdot 10^{7} e$
1500c	$4~\mathrm{cm}$	464	4200	$4.3 \cdot 10^9 e$	$1.1 \cdot 10^7 e$
	$6~\mathrm{cm}$	365	3300	$3.5 \cdot 10^9 e$	$7 \cdot 10^6 \ e$
	$8~\mathrm{cm}$	280	2700	$2.7 \cdot 10^9 e$	$5 \cdot 10^6 \ e$

Table 6. Average flux, peak flux and captured charges per revolution in some satellite orbits

Third, evidently, at 3000 km altitude both the total flux (for x=0) and especially its high-energy part are a few times greater than at 1500 km.

Fourth, and most important: for all orbits in the desirable range of altitudes the charges are quite large as compared with their admissible values; they remain large even behind rather thick walls. It is thus quite necessary to have means to detect and remove the charges during the measurements. Moreover, as seen from the peak values in Table 6 and from time scans of Van Allen charging in orbits of interest (also obtained using the above-mantioned software), at a charging peak when crossing the magnetic equator the time required for the charge on the test bodies to reach its maximum allowable values, as listed above, is a matter of seconds, not minutes. Therefore the charge must be detected and removed as it builds up, on a time scale of seconds.

The detection and measurement of the charge on the test bodies can probably be achieved relatively easily by an array of minute microvoltmeters attached to the inner wall of the experimental chamber.

Several methods for removing positive charge are now being evaluated. A simple and promising method may be to shoot electron beams directly at test bodies. The number of electrons needed is on the order of $10^8/\text{sec}$. Although this approach has the inherent drawback that it requires that an active system must perform correctly for many years, it is simple in principle and will accomplish the goal.

6. Conclusion

Space offers the prospect of quantum leaps in the accuracy of gravitational experiments. Although space is a challenging environment for research, the inherent quiet of space can be exploited to make very accurate determinations of G and other gravitational parameters, providing that care is taken to understand the many physical phenomena in space which have the potential to vitiate accuracy. A distinctive feature of a SEE mission is its capability to perform such determinations simultaneously on multiple parameters, making

it one of the most promising proposals.

To conclude, we enumerate different SEE tests and measurements and show their expected accuracy as currently estimated:

Test/measurement	$Expected\ accuracy$
EP/ISL at a few metres	$2\cdot 10^{-7}$
EP/CD at a few metres	$< 10^{-7} \; (\alpha < 10^{-4})$
EP/ISL at $\sim R_{\oplus}$	$< 10^{-10}$
EP/CD at $\sim R_{\oplus}$	$< 10^{-16} \ (\alpha < 10^{-13})$
G	$3.3 \cdot 10^{-7}$
\dot{G}/G	$< 10^{-13}$ in one year

The last estimate is only tentative; the subject is under study.

Acknowledgement

This work was supported in part by NASA grant # NAG 8-1442. K.A.B. wishes to thank Nikolai V. Kuznetsov for helpful discussions and for providing an access to the SEE2 and SEREIS software.

References

- A.J. Sanders and W.E. Deeds, Phys. Rev. **D** 46, 480 (1992).
- [2] V. de Sabbata, V.N. Melnikov and P.I. Pronin, Progr. Theor. Phys. 88, 623 (1992).
- [3] V.N. Melnikov, Int. J. Theor. Phys. 33, 7, 1569 (1994).
- [4] A.D. Alexeev, K.A. Bronnikov, N.I. Kolosnitsyn, M.Yu. Konstantinov, V.N. Melnikov and A.G. Radynov, *Izmeritel'naya Tekhnika*, 1993, No. 8, 6; No. 9, 3; No. 10, 6; 1994, No. 1, 3; *Int. J. Mod. Phys.* **D** 3, 4, 773 (1994).
- [5] G.T. Gillies, Rep. Progr. Phys. 60, 151 (1997).
- [6] G.G. Luther and W.R. Towler, Phys. Rev. Lett. 48, 121 (1982).
- [7] M.P. Fitzgerald and T.R. Armstrong, "Recent Results for g from MSL Torsion Balance", in: "The Gravitational Constant: Theory and Experiment 200 Years after Cavendish" (23-24 Nov. 1998), Abstracts

- (Cavendish–200 Abstracts), Inst. of Physics, London, 1998.
- [8] J. Schurr, F. Nolting and W. Kündig, Phys. Rev. Lett. 80, 1142 (1998).
- [9] H. Meyer, "Value for G Using Simple Pendulum Suspensions", in: Cavendish-200 Abstracts.
- [10] O.V. Karagioz, V.P. Izmaylov and G.T. Gillies, Grav. & Cosmol. 4, 3, 239 (1998).
- [11] S.J. Richman, T.J. Quinn, C.C. Speake and R.S. Davis, "Determination of G Using the BIPM Torsion Balance", in: Cavendish–200 Abstracts.
- [12] J.P. Schwarz, J.E. Faller, D.S. Robertson and T.M. Niebauer, "The Free-Fall Determination of G, in: Cavendish–200 Abstracts.
- [13] W. Michaelis, "A New Determination of the Gravitational Constant", Bull. Am. Phys. Soc. 40, 2, 976 (1995).
- [14] E. Fischbach and C. Talmage, Mod. Phys. Lett. A4, 2303 (1989); Nature (London) 356, 207 (1992).
- [15] P.G. Roll, R. Krotkov and R.H. Dicke, Ann. Phys. (N.Y.) 26, 442 (1964).
- [16] V.B. Braginsky and V.I. Panov, ZhETF 61, 873 (1971)[Sov. Phys. JETP 34, 463 (1972)].
- [17] E.G. Adelberger, Class. Quantum Grav. 11, A9–A21 (1994).
- [18] Y. Fujii, Nature Phys. Sci. 234, 5 (1971); Ann. Phys. (N.Y.) 69, 494 (1972).
- [19] D.R. Long, Nature (London) 356, 417 (1976); Nuovo Cim. 55B, 252 (1984).
- [20] E.G. Adelberger et al., Phys. Rev. Lett. 59, 8, 849–852 (1987); Phys. Rev. D 42, 10, 3267–3292 (1990).
- [21] E.G. Adelberger, 1997, private communication.
- [22] V. Achilli et al., Nuovo Cim. 112B, 5, 775 (1997).
- [23] E. Fischbach, G.T. Gillies, D.E. Kraus, J.G. Schwan, and C. Talmadge, *Metrologia* 29, 3, 13–260 (1992).
- [24] A. Franklin, "The Rise and Fall of the Fifth Force: Discovery, Pursuit, and Justification in Modern Physics", American Institute of Physics, N.Y., 1993.
- [25] J.-P. Blaser et al., "STEP (Satellite Test of Equivalence Principle): Report on the Phase A Study", ESA/NASA report SCI (93) 4 (March, 1993); "STEP (Satellite Test of Equivalence Principle): Assessment Study", ESA report SCI (94) 5 (May, 1994).
- [26] N.A. Zaitsev and N.I. Kolosnitsyn. *In:* "Experimental Tests of Gravitation Theory", Moscow University Press, 1989, p.38–50 (in Russian).
- [27] K. Nordtvedt, private communication, 1997.
- [28] B.A. Tverskoy, "Dynamics of the Earth's Radiation Belts", Moscow, Nauka, 1968 (in Russian).
- [29] Yu.I. Galperin, L.S. Gorn and B.I. Khazanov, "Radiation Measurments in Space", Moscow, Atomizdat, 1972 (in Russian).
- [30] A.J. Dessler and B.J. O'Brien, "Penetrating Particle Radiation", in: "Satellite Environment Handbook", 2nd edition, ed. F.S. Johnson, Stanford University Press, Stanford, CA, 1965, p. 53–92.

- [31] W.N. Hess, "The Radiation Belt and Magnetosphere", Ginn Blaisdell, Waltham, MA, 1968.
- [32] V.F. Bashkirov and M.I. Panasiuk, "Dynamics of the Trapped Radiation Environment at Low Altitude Region of the Earth's Magnetosphere". Workshop "Space Radiation Environment Modelling: New Phenomena and Approaches", Oct. 7–9, 1997: Program and Abstracts, p. 1.2.
- [33] V.F. Bashkirov, N.V. Kuznetsov and R.A. Nymmik, "Information System for Evaluation of Space Radiation Environment and Radiation Effects on Spacecraft", ibid., p. 4.8.
- [34] V.F. Bashkirov and M.I. Panasiuk, Kosmicheskiye Issledovaniya (Space Research), 36, 4, 359–368 (1998).
- [35] D. Bilitza, "Solar-Terrestrial Models and Application Software", Planet. Space Sci. 40, 4, 541–579 (1992).

This figure "PIC1.GIF" is available in "GIF" format from:

http://arxiv.org/ps/gr-qc/0002088v1

This figure "PIC2.GIF" is available in "GIF" format from: http://arxiv.org/ps/gr-qc/0002088v1 This figure "PIC3.GIF" is available in "GIF" format from: http://arxiv.org/ps/gr-qc/0002088v1